

Seasonal changes in river water pollution levels induce oxidative stress and DNA damage in human keratinocytes

Nebiye Pelin Türker*, Pınar Altınoluk Mimiroğlu

Trakya University, Technology Research and Development Centre, Edirne, Türkiye

Cite this article as: Türker, N. P., & Altınoluk Mimiroğlu, P. (2026). Seasonal changes in river water pollution levels induce oxidative stress and DNA damage in human keratinocytes. *Trakya University Journal of Natural Sciences*, 27(1), 76–87. <https://doi.org/10.23902/trkjnat.2025108>

Abstract

Background: Seasonal heavy metal pollution of river waters poses a significant risk to environmental and human health; yet its biological effects are often insufficiently characterized.

Aims: The aim of this study was to investigate the seasonal variations in river water pollution and to evaluate the associated cytotoxic, oxidative, and genotoxic effects of these waters on human keratinocytes using an integrated *in vitro* approach.

Methods: This study collected river water samples during the four seasons and evaluated their cytotoxic and genotoxic impacts in human keratinocytes using an integrated *in vitro* approach. The cells were exposed to the samples for 24 and 48 h. Cytotoxicity was assessed via the 3-(4,5-dimethylthiazol-2-yl)-2,5 diphenyl tetrazolium bromide assay, elemental accumulation by inductively coupled plasma–mass spectrometry, and oxidative and genotoxic responses by assessing reactive oxygen species (ROS) and 8-hydroxy-2'-deoxyguanosine (8-OHdG) levels.

Results: All samples induced time- and season-dependent cytotoxicity, whereas control cells were unaffected. Autumn-collected samples exhibited the maximal cytotoxicity, with cell mortality ranging from 38.94% to 80.09% at 24 h and increasing to 56.97%–81.03% at 48 h. Spring-collected samples induced the second-highest lethality, with cell death reaching $\leq 90.03\%$ at 48 h. Enhanced cytotoxicity was associated with elevated cellular levels of Fe, Al, Cr, Ni, Ca, and Sr at 24 h and Ti, Mn, Zn, Cu, and P at 48 h, indicating rapid uptake and delayed accumulation patterns. River water exposure also significantly increased ROS generation ($p < 0.005$) and 8-OHdG

Özet

Dayanak: Nehir sularının mevsimsel ağır metal kirliliği, çevre ve insan sağlığı için önemli bir risk oluşturmaktadır ancak biyolojik etkileri genellikle yeterince tanımlanmamıştır.

Amaçlar: Bu çalışmanın amacı, nehir suyu kirliliğindeki mevsimsel değişimleri araştırmak ve bu suların insan keratinositleri üzerindeki ilişkili sitotoksik, oksidatif ve genotoksik etkilerini bütünlük bir *in vitro* yaklaşım kullanarak değerlendirmektir.

Yöntemler: Bu çalışmada, dört mevsim boyunca nehir suyu örnekleri toplanmış ve entegre bir *in vitro* yaklaşım kullanılarak insan keratinositlerinde sitotoksik ve genotoksik etkileri değerlendirilmiştir. Hücreler, 24 ve 48 saat boyunca örneklerle temas ettirilmiştir. Sitotoksikite, 3-(4,5-dimetiltiazol-2-il)-2,5-difeniltetrazolyum bromür testi ile, element birikimi induktif eşleşmiş plazma–kütle spektrometrisi ile ve oksidatif ve genotoksik tepkiler reaktif oksijen türleri (ROS) ve 8-hidroksi-2'-deoksiguanozin (8-OHdG) düzeyleri değerlendirilerek ölçülmüştür.

Bulgular: Tüm numuneler zamana ve mevsime bağlı sitotoksisiteye neden olurken, kontrol hücreleri etkilenmemiştir. Sonbaharda toplanan numuneler maksimum sitotoksisite göstermiş, hücre ölüm oranı 24 saatte %38,94 ile %80,09 arasında değişmiş ve 48 saatte %56,97 ile %81,03'e yükselmiştir. İlkbaharda toplanan örnekler, 48 saatte hücre ölümünün $\leq 90,03\%$ 'e ulaşmasıyla ikinci en yüksek ölüm oranını indükledi. Artan sitotoksisite, 24 saatte Fe, Al, Cr, Ni, Ca ve Sr ve 48 saatte Ti, Mn, Zn, Cu ve P hücre seviyelerindeki artışla ilişkililiydi, bu da hızlı alım ve gecikmiş birikim modellerini gösteriyordu. Nehir suyuna maruz kalma, özellikle sonbahar ve ilkbahar örneklerinde,

Edited by: Bülent Yorulmaz

*Corresponding Author: Nebiye Pelin Türker, E-mail: npelinturker@trakya.edu.tr

ORCID iDs of the author(s): NPT. 0000-0001-6060-3557; PAM. 0000-0002-8524-0972



Received: 28 October 2025, Accepted: 31 December 2025, Epub: 29 January 2026, Published: 24 April 2026



Copyright© 2026 The Author(s). Published by Galenos Publishing House on behalf of Trakya University. Licensed under a Creative Commons Attribution (CC BY) 4.0 International License.



levels, particularly by autumn and spring samples, demonstrating cumulative oxidative DNA damage.

Conclusion: These findings indicate that seasonal river water pollution induces oxidative stress mediated cytotoxicity and genotoxicity in human keratinocytes. The study underscores the necessity of incorporating biological endpoints into routine water quality monitoring to better assess health risks associated with contaminated freshwater systems.

Keywords: River water quality, human keratinocyte cells, reactive oxygen species, oxidative DNA damage, seasonal variation

Introduction

Water pollution is a major environmental challenge driven by industrialization, agriculture, environmental factors, insufficient freshwater resources, and inadequate sewage treatment systems. Industrial activities constitute a dominant source of aquatic contamination, particularly effluents released from textile, food processing, pulp and paper, iron, and steel factories; distilleries and tanneries; and nuclear power plants (Chowdhary et al., 2019). These industries discharge wastewater containing volatile organic compounds, toxic chemicals, inorganic pollutants, and hazardous solvents, often without sufficient treatment. They also contaminate surface waters with heavy metals (HMs), the most prevalent being chromium, cadmium, and arsenic (Chen et al., 2019). For example, anthropogenic activities have resulted in extensive hexavalent chromium pollution in the central regions of the Loess Plateau, China (Ge et al., 2020). With accelerating urbanization, the volume and complexity of industrial wastewater discharges continue to increase (Wu et al., 2020).

Agricultural activities represent another significant contributor to water pollution, primarily through runoff containing organic waste, nitrogen-based fertilizers, and pesticides. Cropping systems release pesticides, soil sediments, nitrates, phosphates, salts, and pathogens into aquatic environments, degrading the ecosystem and posing potential risks to human health (Parris, 2011). Such pollution severely affects freshwater ecosystems (Moss, 2008) and poses additional concerns related to food safety and HM accumulation (Lu et al., 2015). In parallel, environmental factors can also influence water quality; elevated levels of trace elements, sodium, and salinity are associated with poor river water quality in regions such as the Loess Plateau (Xiao et al., 2019). In many developing countries, inadequate sewage treatment infrastructure and insufficient investment in water supply systems further exacerbate contamination-associated problems, enhancing the exposure to industrial chemicals, HMs, and algal toxins (Wu et al., 1999).

The impacts of contaminated water on human health are well documented, with polluted drinking and surface waters contributing to gastrointestinal, infectious, and chronic diseases worldwide. The use of water filtration systems or desalinated water in households markedly reduces the incidence of diarrheal diseases compared to untreated municipal water (Yassin et al., 2006). In contrast, the consumption of tap water is associated

ROS oluşumunu ($p < 0,005$) ve 8-OHdG seviyelerini önemli ölçüde artırarak, kümülatif oksidatif DNA hasarını ortaya koydu.

Sonuç: Bu bulgular, nehir suyunun mevsimsel ağır metal kirliliğinin, insan keratinositlerinde oksidatif stres aracılı sitotoksinite ve genotoksiniteye neden olduğunu göstermektedir. Bu çalışma, kirlenmiş tatlı su sistemleriyle ilişkili sağlık risklerini daha iyi değerlendirmek için rutin su kalitesi izleme protokollerine biyolojik son noktaların dahil edilmesinin gerekliliğini vurgulamaktadır.

with an increase in gastrointestinal disorders (Payment et al., 1997). Beyond systemic health effects, recent research emphasizes that water pollution levels exhibit pronounced seasonal and spatial variability, which directly influences the concentrations of contaminants and associated risks. Hammoumi et al. (2024) reported significant seasonal quality fluctuations in the surface water of the Nador Canal; water quality was lower during the summer due to combined natural and anthropogenic factors, including agricultural runoff and industrial discharges. Similarly, in Anambra State, Nigeria, Amaechi et al. (2025) observed elevated levels of Cd, Pb, Zn, and Cu in river water during the dry season, primarily driven by industrial effluents, with a partial dilution of these contaminants occurring during the wet season. At the cell level, exposure to HM-contaminated water induces oxidative stress and inflammatory responses, leading to tissue damage and increasing susceptibility to chronic diseases. Kolawole et al. (2025) demonstrated that cadmium, lead, and arsenic induce a remarkable elevation in oxidative stress biomarkers and inflammatory mediators, underscoring a mechanistic link between environmental contamination and adverse biological outcomes. Water pollution is also associated with dermatological disorders, including melanosis, keratosis, hair loss, scabies, and skin cancer, particularly in populations using contaminated surface waters for drinking purposes. Chronic exposure to arsenic-contaminated water causes severe skin-related health effects (Kazi et al., 2009), while polluted rivers and industrial waters increase the incidence of scabies and skin cancer (Arif et al., 2020; Hanif et al., 2020). Meta-analyses further support the association between polluted aquatic environments and skin conditions such as erythema and pruritus (Fleisher & Kay, 2006; Yau et al., 2009).

Despite this extensive body of epidemiological and chemical evidence, experimental findings directly assessing the effects of river water samples on healthy human skin cells remain limited. A small number of *in vitro* studies have evaluated the biological toxicity of surface or river waters using aquatic organisms or non-human models. For instance, Amaechi et al. (2025) demonstrated season-dependent cytotoxic effects of river water samples on fish-derived cell lines, attributing toxicity to elevated HM loads, while genotoxic endpoints were not examined. Similarly, Hammoumi et al. (2024) assessed seasonal variations in surface water quality and reported reduced biological quality during summer months; however, their evaluation was restricted to physicochemical parameters without cell-based toxicity or DNA

damage analyses. Overall, existing *in vitro* investigations have predominantly focused on non-human models, have been limited to single locations or seasons, and have largely assessed cytotoxicity alone, leaving genotoxic outcomes and human-relevant dermal exposure risks insufficiently characterized. To address this gap, the present study focuses on the Meriç–Ergene River Basin, a region extensively impacted by industrial discharges, agricultural runoff, and urbanization. Water samples were collected from nine strategically selected stations along the Meriç, Ergene, and Tunca rivers to capture spatial variability, hydrological characteristics, and pollution gradients. Using a healthy human keratinocyte line, we evaluated the cytotoxic effects (on cell viability) and genotoxic potential of the collected samples. By integrating spatially distributed environmental sampling with human-relevant *in vitro* assays, this study provides biomonitoring-based evidence that directly links surface water pollution to potential dermal health risks, extending beyond conventional ecological or chemical assessments.

Materials and Methods

Sampling Stations and Transport of Samples

Water samples were collected from three major rivers the Meriç (Maritsa), Ergene, and Tunca rivers located in northwestern Türkiye. The Meriç River forms part of the border between Türkiye and Greece and flows southward into the Aegean Sea, while the Ergene and Tunca rivers are important tributaries draining agricultural and industrial regions before discharging into the Meriç River. At each station, water from underneath the surface was collected, against the flow, and stored in 2 L brown glass bottles. Samples were transported to the laboratory under cold-chain conditions. The sampling station locations are detailed in Table 1. *In situ* measurements of the routine physicochemical parameters of the water at each sampling station, including temperature (°C), pH, and electrical conductivity (µS/cm), were performed at the time of collection with a portable multi-parameter water quality meter calibrated according to the manufacturer's instructions. These parameters were recorded to characterize the prevalent environmental conditions at the time of sampling and support an interpretation of the findings of the subsequent biological and toxicological analyses.

Table 1. Sampling station details.

Rivers	Stations	Locations
Meriç River	Station 1 (M1)	41°39'44"N, 26°33'06"E
	Station 2 (M2)	41°37'32"N, 26°34'48"E
	Station 3 (M3)	41°29'12"N, 26°36'08"E
Ergene River	Station 1 (E1)	41°18'15"N, 27°26'40"E
	Station 2 (E2)	41°20'06"N, 26°55'19"E
	Station 3 (E3)	41°14'45"N, 26°37'04"E
Tunca River	Station 1 (T1)	41°45'34"N, 26°33'32"E
	Station 2 (T2)	41°41'08"N, 26°33'15"E
	Station 3 (T3)	41°40'02"N, 26°33'14"E

Cell Culture

Human keratinocyte cell line (HaCaT) was cultured in Dulbecco's Modified Eagle Medium: Ham's F-12 medium supplemented with 1% L-glutamine, 5% fetal bovine serum, and 1% penicillin/streptomycin. The cells were placed in a cell culture incubator and cultivated at 37 °C under 5% CO₂ and 95% humidity. They were subcultured upon reaching an 80%–90% confluency.

Cytotoxicity Determination via 3-(4,5-dimethylthiazol-2-yl)-2,5 diphenyl tetrazolium bromide (MTT) Assay

The cytotoxic impacts of river water on HaCaT cells were evaluated using the MTT assay. Cells were seeded in a 96-well plate at a density of 2×10^4 cells/well in 180 µL of medium. After incubation for 24 h, the cells were exposed to river water applied at nine concentrations: 100%, 50%, 25%, 12.5%, 6.25%, 3%, 1.5%, 0.75%, and 0.39%, for 24 and 48 h. Then, 20 µL of 5 mg/mL MTT solution (in phosphate-buffered saline) was added to each well. All experiments were conducted in four replicates (n = 4). The plates were incubated for another 2 h, and the formazan crystals formed were dissolved in 100–200 µL of dimethyl sulfoxide. The OD₅₇₀ was measured, and cell viability and mortality were calculated by applying the formulae-formulas:

$$\text{Viability (\%)} = (\text{Experimental absorbance}/\text{Control absorbance}) \times 100$$

$$\text{Mortality (\%)} = 100 - \text{Viability (\%)}$$

Determination of Cell Elemental Concentrations Employing Inductively Coupled Plasma-Mass Spectrometry (ICP-MS)

HaCaT cells were seeded into 24-well culture plates at a density of 1×10^5 cells/well and incubated at 37 °C for 24 h in a humidified atmosphere containing 5% CO₂. Following cell attachment, the culture medium was replaced with river water samples, to which the cells were exposed for 24 and 48 h. These durations were selected based on the cytotoxicity thresholds determined via the MTT assay to avoid excessive cell death. After exposure, the cells were harvested and acid digested for elemental analyses with 65% ultrapure HNO₃ (trace metal grade), using a controlled combustion/digestion procedure until complete mineralization. Subsequently, the digested samples were diluted to appropriate volumes with ultrapure water before analysis. Cell elemental concentrations were quantified using a 7700 series ICP-MS (Agilent Technologies, Inc., CA, USA). Calibration curves were plotted using certified multi-element standard reference (high-purity) solutions in the range of 0–1000 ppb prepared by serial dilution. Calibration standards were used at five concentrations, covering the samples' expected range. Curve linearity was evaluated, and correlation coefficients (R²) were verified to ensure acceptable performance levels. Quality control samples were employed to verify calibration validity and signal consistency before proceeding with sample measurements. Calibration standards were measured periodically to ensure analytical accuracy and instrument stability. Data obtained only under stabilized and calibrated conditions were included in the final analysis. Instrument operating parameters, including plasma conditions, nebulizer settings, and acquisition modes,

are detailed in Table 2. All samples were analyzed in triplicate ($n = 3$), and elemental levels were expressed as mean values. Statistical analyses were employed to identify elements with significant variations between experimental groups. Subsequently, principal component analysis (PCA) was applied to such elements to evaluate the patterns in elemental concentration variations and potential exposure duration-related clustering.

Table 2. ICP-MS parameters.

Instrument parameter	Operating conditions
Plasma gas	Argon, ultrahigh purity, 99.999%
Carrier gas	Helium, ultrahigh purity, 99.999%
Plasma gas pressure	500–700 kPa
Carrier gas pressure	90–130 kPa
Chiller temperature	18 °C
Carrier gas flow rate	1.05 L/min
Radio frequency power	1550 Watt
Radio frequency matching	1.80 V
Cones	Ni sampling cone for the X-lens
Nebulizer pump	0.1 rps

ICP-MS = inductively coupled plasma–mass spectrometry.

Assessment of Reactive Oxygen Species (ROS) Levels

HaCaT cells were seeded in 24-well plates at a density of 1×10^5 cells per well and incubated for 24 hours at 37 °C and under 5% CO₂. Water samples at toxic dosages (ascertained utilizing the MTT assay) were applied to the cells, and incubated for 24–48 h. Experiments were performed in three replicates ($n = 3$). The ROS levels of these cells were measured spectrophotometrically with a commercial ROS detection kit (Shanghai Sunred Biological Technology Co., Ltd., Shanghai, China); the assay procedure is outlined in Table 3. Statistical significance (Sig.) was evaluated using analysis of variance (ANOVA), followed by Student's t-test for pairwise comparisons. Differences between the mean ROS assay expression values obtained were assessed employing Student's t-test.

Table 3. Protocol for ROS detection using an ELISA kit.

Operation steps	Temperature/time
Standard preparation and reagents	-
Sample preparation	20 min, centrifuge the samples at 2000–3000 rpm
Adding enzyme-labeled antibodies to samples and standards	60 min, 37 °C
Washing process	5 × 100 µL
Adding the chromogenic reagents	10 min, 37 °C
Adding the stop solution	15 min, 50 µL
Measuring optical density values and calculations	Within 10 minutes, 450 nm was detected.

ELISA = Enzyme-Linked Immunosorbent Assay; ROS = reactive oxygen species.

Assessment of Oxidative DNA Damage using 8-Hydroxy-2'-Deoxyguanosine (8-OHdG) as a Biomarker

HaCaT cells were seeded in 24-well plates at a density of 1×10^5 cells per well and incubated for 24 h at 37 °C under 5% CO₂. DNA was extracted from the cells after exposure to toxic doses of contaminated river water for 24 and 48 h. Oxidative DNA damage was assessed utilizing reactions catalyzed by Nuclease P and phosphatase. Oxidative stress-related markers were quantified using liquid chromatography-tandem mass spectrometry (LC-MS/MS) on a Jet Stream 6460 Triple Quadrupole instrument (Agilent Technologies). The analysis parameters are provided in Table 4.

Table 4. Parameters of LC-MS/MS-based oxidative DNA damage analysis.

Mobile phase	A: Ultrapure water containing 5 mM ammonium formate B: Methanol containing 5 mM ammonium formate		
Column	Poroshell EC-C18 (3.0 × 150 mm, 3.5 Micron)		
Column temperature	35 °C		
Injection volume	5 µL		
Flow rate	0.6 mL/min		
Gradient program	Time (min)	A (%)	B (%)
	0.00	95.0	5.0
	0.70	95.0	5.0
	1.70	5.0	95.0
	4.50	5.0	95.0
	5.00	95.0	5.0
	10.00	95.0	5.0

LC-MS/MS = liquid chromatography-tandem mass spectrometry.

Statistical Analysis

Probit analysis was applied to the MTT assay results to determine the 50% lethal dose (LD₅₀), in accordance with the Turkish Standards Institute (TSE) and ISO 10993-5 guidelines. Prior to parametric analyses, the assumption of homogeneity of variances was assessed using Levene's test. When variance homogeneity was satisfied ($p > 0.05$), parametric tests were applied. Comparisons involving more than two groups (e.g., seasonal or station-based differences in cytotoxicity, ROS production, elemental accumulation, and 8-OHdG levels) were evaluated using one-way ANOVA. When significant differences were detected, Tukey's post hoc test was applied to identify pairwise group differences. In cases where the assumption of homogeneity of variances was violated, Welch's ANOVA followed by the Games–Howell post hoc test was used. Comparisons between two groups were performed using Student's t-test or Welch's t-test, as appropriate. PCA was used to explore patterns in ICP-MS-derived elemental profiles. Correlations between 8-OHdG levels were assessed using Pearson's or Spearman's correlation analyses, depending on data

distribution. Statistical analyses were performed using XLSTAT, GraphPad Prism, and SPSS v25.0. A $p < 0.05$ was considered statistically significant.

Results

Physicochemical Characteristics of the River Water Samples

The physicochemical properties of the river water samples, including temperature, pH, and electrical conductivity, measured at the time of sampling, are summarized in Table 5. Pronounced seasonal variations were observed in these parameters across sampling stations, with temperature being minimum during winter (8.0–12.0 °C) and maximum during the summer (27.0–31.0 °C). The pH values remained slightly alkaline, ranging from 7.36 to 8.33, throughout the study period, and exhibited only minor seasonal fluctuations. In contrast, electrical conductivity exhibited pronounced spatial variability, with substantially elevated values recorded at station E (2200–4300 $\mu\text{S}/\text{cm}$) and the least at stations M and T (339–923 $\mu\text{S}/\text{cm}$), likely reflecting differences in hydrological conditions and local anthropogenic influences among the three rivers. Overall, electrical conductivity values were higher during autumn and winter than in spring and summer. These baseline physicochemical characteristics provide essential contextual information for the interpretation of subsequent cell and toxicological findings.

Analysis of Cytotoxicity Results

The cytotoxicities of various river water samples were evaluated, and the findings are presented in Figure 1. The results demonstrated an obvious time-dependent increase in mortality rates among most treatment groups compared to the control (non-exposed) group, which exhibited 0% mortality. The asterisk (*) above the bars indicates statistically significant variations between the two groups. The TSE ISO 10993-5 standard considers a test material to be cytotoxic if it causes >30% cell mortality (<70% viability). A majority of the samples were classified as toxic, based on this

guideline. Such cytotoxicity was most pronounced after 48 h of exposure and was particularly severe in the samples collected during Autumn (e.g., T1–T3, M1–M3, and E1–E3), with mortality rates consistently >50%. These findings confirm the marked presence of cytotoxic agents in river water, with the maximum toxicity induced by the Autumn samples at the 48 h time point (Figure 1 and Table 6).

Results of the Intracellular Element Levels Determination

This study provides evidence with robust statistical Sig. that the concentrations of trace elements within cells exposed to river water are highly sensitive to sampling location and exposure duration. PCA demonstrated that, at 24 h and 48 h of exposure, a majority of the total variance was explained by the first PC1, indicating that dataset variability was primarily driven by differences in element accumulation levels among exposure groups. PCA further revealed robust positive correlations among Fe, Al, Ca, Cr, and Ni at 24 h and among Ti, Mn, and P at 48 h. These observations suggest that such elements either originate from a common environmental source or are taken up by cells through shared or closely related biochemical pathways. Moreover, a clear and statistically significant separation of the E group from all others (prominent main effect, $p < 0.001$) confirms that source-specific differences in river water composition are the primary determinants of variations in intracellular element accumulation levels. Extension of exposure duration from 24 to 48 h identified two distinct accumulation dynamics. The absence of statistically significant variations in Fe, Al, Cr, and Ni contents at 24 and 48 h indicates rapid intracellular saturation or cell-regulatory mechanisms achieving equilibrium within the initial 24 h of exposure. In contrast, the Ti, Mn, Zn, Cu, and P contents elevated significantly at 48 h, suggesting that these elements may require prolonged periods of exposure for accumulation or follow slower uptake kinetics. A particularly crucial finding was the pronounced time–season interaction observed with Ca and Sr. Their concentrations increased markedly from 24 to 48 h, with those of Ca and Sr elevating by 1.7–2.58-fold and 1.17–2.10-fold, respectively. Such variability depended on the season, indicating that Ca and Sr accumulation was remarkably

Table 5. Seasonal changes in the physicochemical parameters of river water samples.

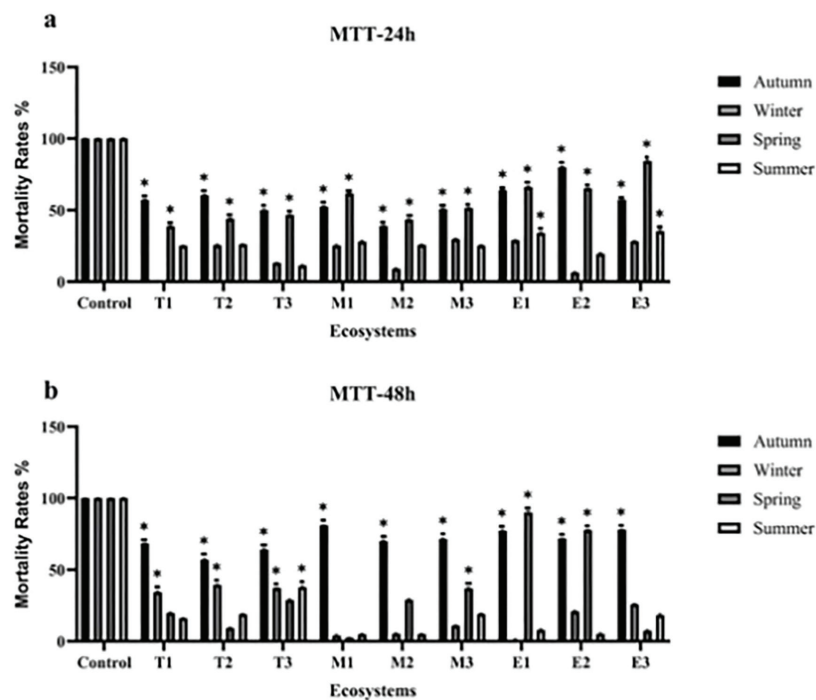
	Autumn			Winter			Spring			Summer		
	Temp. (°C)	pH	EC ($\mu\text{S}/\text{cm}$)	Temp. (°C)	pH	EC ($\mu\text{S}/\text{cm}$)	Temp. (°C)	pH	EC ($\mu\text{S}/\text{cm}$)	Temp. (°C)	pH	EC ($\mu\text{S}/\text{cm}$)
E1	18.0	7.83	3910	10.0	7.81	2410	21.0	7.82	2200	31.0	8.01	2270
E2	18.0	7.90	4300	12.0	7.81	2760	23.0	7.74	2260	30.0	7.99	2330
E3	19.0	7.84	3910	10.0	7.59	2430	21.0	7.68	2250	30.0	8.00	2290
M1	14.0	8.04	526	9.0	8.33	339	23.0	8.23	388	27.5	8.04	493
M2	15.0	8.01	411	8.0	8.27	344	24.0	8.13	382	28.0	8.07	499
M3	17.0	7.79	574	10.0	7.36	536	25.0	7.45	438	27.5	8.06	504
T1	12.0	8.06	900	8.0	8.16	827	22.0	7.78	714	27.0	7.80	834
T2	14.0	7.93	923	8.5	8.13	807	22.0	7.77	712	29.0	7.39	887
T3	14.0	7.65	913	8.0	8.18	822	23.0	7.72	724	28.0	7.87	892

EC = electrical conductivity; Temp. = temperature.

Table 6. Percentage mortality rates after 24 and 48 hours of exposure to river water (n = 4, % mean \pm SD).

Ecosystem	Autumn		Winter		Spring		Summer	
	24 h	48 h	24 h	48 h	24 h	48 h	24 h	48 h
T1	57.18 \pm 0.35	68.34 \pm 0.28	0.52 \pm 0.42	34.28 \pm 0.47	38.69 \pm 0.45	19.79 \pm 0.45	25.16 \pm 0.24	16.17 \pm 0.24
T2	60.56 \pm 0.45	56.97 \pm 0.74	25.62 \pm 0.65	39.38 \pm 0.66	44.07 \pm 0.52	9.26 \pm 0.52	26.20 \pm 0.36	19.07 \pm 0.36
T3	50.01 \pm 0.96	64.06 \pm 0.96	13.22 \pm 0.24	37.15 \pm 0.25	46.65 \pm 0.68	28.95 \pm 0.68	11.33 \pm 0.74	37.86 \pm 0.74
M1	52.51 \pm 0.45	81.03 \pm 0.15	25.31 \pm 0.74	4.01 \pm 0.74	61.73 \pm 0.14	2.55 \pm 0.14	28.11 \pm 0.53	4.89 \pm 0.52
M2	38.94 \pm 0.75	70.09 \pm 0.52	9.03 \pm 0.62	5.29 \pm 0.63	43.47 \pm 0.74	29.01 \pm 0.74	25.76 \pm 0.45	5.01 \pm 0.45
M3	50.79 \pm 0.68	71.43 \pm 0.58	29.77 \pm 0.52	10.93 \pm 0.52	51.50 \pm 0.63	37.12 \pm 0.63	25.31 \pm 0.38	19.16 \pm 0.38
E1	64.06 \pm 0.35	77.2 \pm 0.65	28.95 \pm 0.54	1.15 \pm 0.54	66.14 \pm 0.85	90.03 \pm 0.85	34.09 \pm 0.65	7.99 \pm 0.65
E2	80.09 \pm 0.54	71.78 \pm 0.24	6.47 \pm 0.62	20.94 \pm 0.62	65.26 \pm 0.25	77.74 \pm 0.25	19.61 \pm 0.75	5.22 \pm 0.75
E3	57.30 \pm 0.65	77.87 \pm 0.45	28.27 \pm 0.34	25.91 \pm 0.34	84.31 \pm 0.78	7.26 \pm 0.78	35.36 \pm 0.98	18.32 \pm 0.98

SD = standard deviation.

**Figure 1.** Assessment of river water-induced cytotoxicity in HaCaT cells across ecosystems and seasons: MTT assay results. (a) MTT-24 h results (top panel). The top panel illustrates the viability rates (%) in HaCaT cells after 24 h of exposure to water samples. Exposure to the waters of most river ecosystems—T1–T3, M1–M3, and E1–E3—markedly reduced cell viability compared to the control, with mortality rates clustering between 25% and 75%. (b) MTT-48 h results (Bottom Panel). The bottom panel presents the cell viability after 48 h of exposure. It indicates a time-dependent increase in cytotoxicity, with generally elevated mortality rates observed across ecosystems compared to 24 h. The asterisk symbol (*) indicates that the viability rates between the corresponding groups and seasons differed with statistical Sig. ($p < 0.05$) from the control group.

Key findings: The graph confirms a significant ecosystem–collection time–season interaction, as the E group samples consistently induced the maximum mortality rates, particularly during Autumn and Winter, indicating that the source of water (E) and the season of collection are major determinants of toxicity.

HaCaT = human keratinocyte cell line; MTT = 3-(4,5-dimethylthiazol-2-yl)-2,5 diphenyl tetrazolium bromide; Sig. = significance.

influenced by exposure duration and environmental conditions, positioning these elements as plausible, high-sensitivity biological indicators of seasonal and environmental dynamics. In conclusion, the findings of the combined PCA and variance analyses demonstrate that the river water environments investigated were

heterogeneous regarding trace element composition and that cell responses differed prominently depending on the water source. These findings underscore the critical nature of including exposure duration and seasonal variability in environmental pollution risk assessments and toxicological evaluations (Figure 2).

ROS-Mediated Oxidative Stress and DNA Damage Assessed by Measuring 8-OHdG Levels

The differences in ROS levels within the HaCaT cells exposed or not exposed to river water for 24 and 48 h were evaluated using the independent samples t-test, preceded by Levene's test for equal variances. As most groups showed two-tailed Sig. values >0.05 , the assumption of equal variances was generally met. The t-test results, specifically the Sig. values, revealed that ROS levels of most treated group cells differed with high Sig. compared to the control group ones (Sig. 0.005). The variations among most samples from the E, M, and T ecosystems across seasons were statistically significant (*). ROS levels induced by only three spring samples, E2-Spring (Sig. = 0.695), M1-Spring (Sig. = 0.251), and T3-Spring (Sig. = 0.070) did not differ with statistical Sig. from the contents of control group cells at the tested time points. These

trends suggest that spring-collected samples induced a negligible oxidative stress response in HaCaT cells (Figure 3, Table 7).

As expected, control group cells demonstrated the lowest 8-OHdG levels at both 24 and 48 h of treatment, indicating minimal DNA damage under normal cell culture conditions. In contrast, cells of all groups exposed to river water exhibited markedly elevated 8-OHdG levels compared to the control group cells. Such an increase confirms that pollutants present in river water induced oxidative stress and consequent DNA damage in the HaCaT cells.

The overall trend indicated an increase in DNA damage with prolonged pollutant exposure. As illustrated, cell 8-OHdG levels were higher at 48 h compared to 24 h upon treatment with water collected from several locations, e.g., E1-Winter, E2-Winter, M1-Winter, M2-Spring, and T2-Winter. However, DNA damage

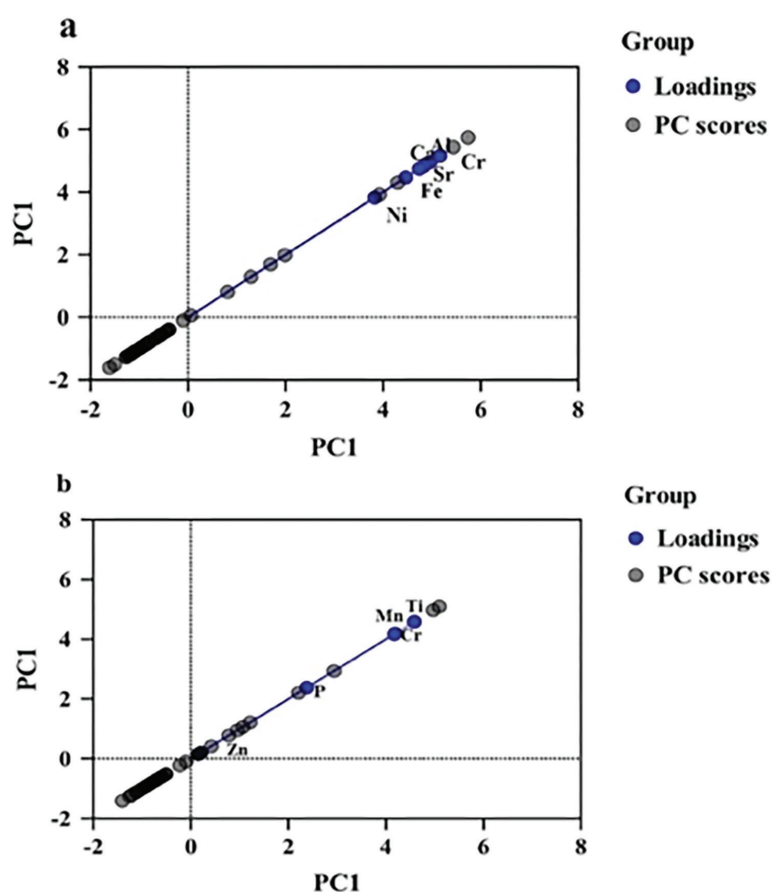


Figure 2. PCA of the intracellular accumulation of elements at 24 and 48 h of exposure to river water. (a) 24 h Exposure: Identification of the Core Accumulation Group and Significant Group Separation: The 24 h PCA biplot demonstrates that Fe, Al, Ca, Cr, and Ni exhibit strong correlations (the Core Accumulation Group) and load heavily onto the PC1 axis. This trend proves that source-derived differences are the dominant factors determining element accumulation. The clear separation of group scores along the PC1 axis confirms that river water exposure resulted in statistically significant variations in element uptake across groups. (b) 48 h Exposure: Impact of Time on Sensitive Element Dynamics: The 48 h PCA biplot indicates an expansion in the element group to include Ti, Mn, and P, which were markedly elevated at 48 h. This observation, combined with the finding that Fe, Al, Cr, and Ni contents did not show statistically significant differences at 24 and 48 h, highlights varying kinetic uptake rates. Critically, the PCA supports Ca and Sr displaying the maximum sensitivity, demonstrating statistically significant and season-dependent fold-changes between their levels at 24 and 48 h, marking them as the biological indicators most reactive to prolonged exposure.

PCA = principal component analysis.

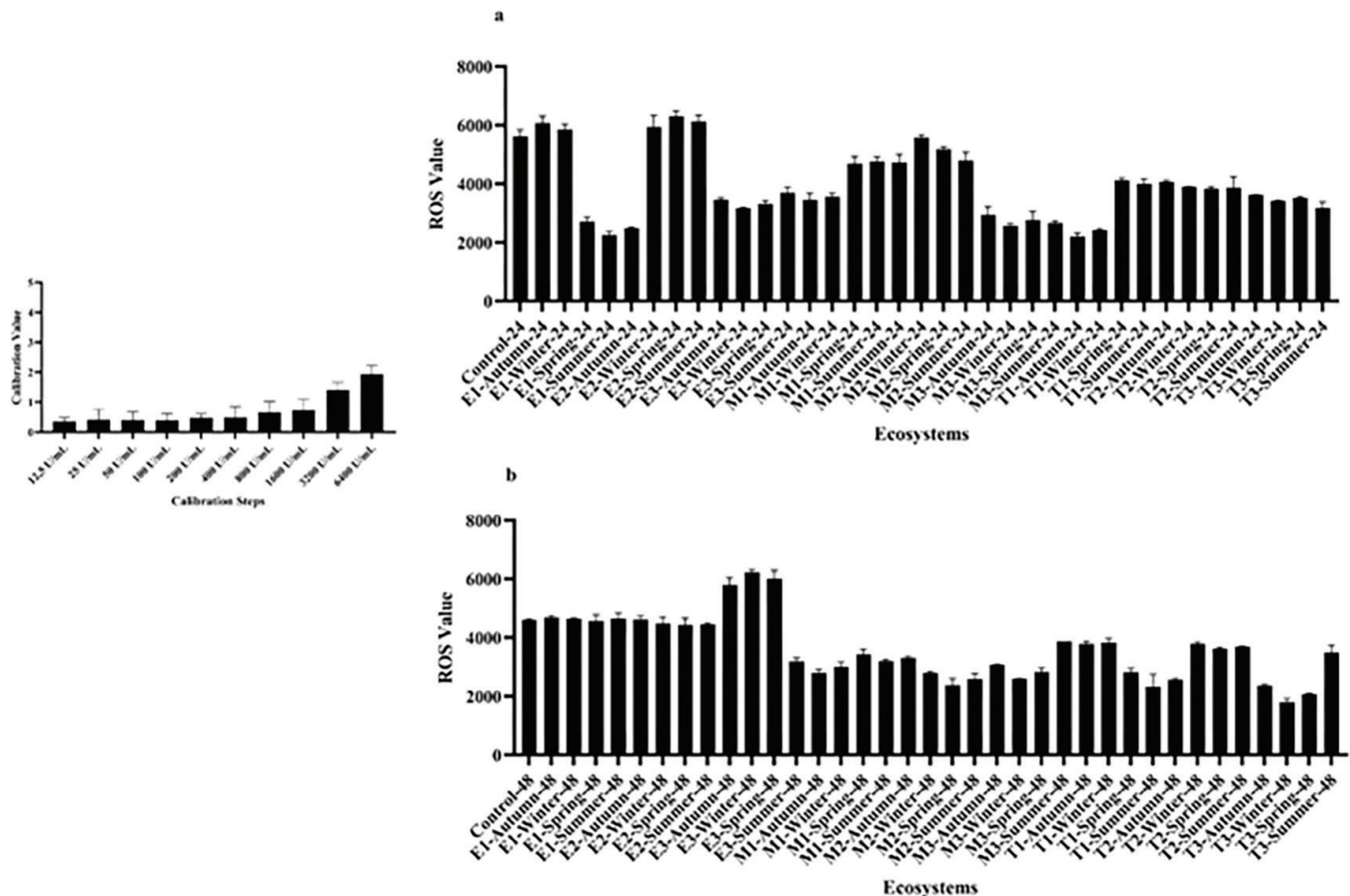


Figure 3. ROS production in HaCaT cells following exposure to river water: Time- and ecosystem-dependent stress.

(a) ROS Production at 24 h (top panel). The top panel presents the ROS contents after 24 h of exposure. It indicates a significant ecosystem–time–season interaction, with particularly severe oxidative stress observed in the E groups (E1, E2, and E3) during all seasons relative to the control as well as the T and M groups. This observation suggests that the water from the E ecosystem induced an immediate and robust oxidative response. (b) ROS Production at 48 h (bottom panel). The bottom panel shows the ROS values after 48 h of exposure to river water. It indicates a temporal moderation of the oxidative response, where the initially high ROS levels observed in the E groups at 24 h either normalized or slightly decreased, but slightly increased in certain M and T groups. The maintenance of moderate ROS levels within most groups at 48 h suggests cell adaptation or establishment of a novel oxidative equilibrium under continuous environmental stress.

HaCaT = human keratinocyte cell line; ROS = reactive oxygen species.

induced by water collected from a few locations declined at 48 h relative to 24 h (e.g., E1-Autumn). This observation suggests activation of DNA repair mechanisms or extensive cell death at 48 h, which reduced the number of viable cells or DNA available for measurement. The T2-Spring group cells exhibited the maximal 8-OHdG levels at 48 h (~18), indicating the most severe DNA damage and suggesting that the pollutants at this location, as well as the collection season exerted the strongest genotoxicity. Conversely, the E1-Autumn group cells showed the highest 8-OHdG contents at 24 h (~13.5), implying a rapid and potent induction of oxidative stress by river water during autumn. In winter group cells, particularly the M2-Winter and T2-Winter group ones, a pronounced elevation in 8-OHdG levels was detected at 48 h (Figure 4). Overall, the severity and duration of oxidative stress–induced DNA damage may vary remarkably depending on exposure time generally increasing at 48 h as well as on the river ecosystem type and seasonal conditions.

Discussion

The present study evaluated the toxicological effects of river water with seasonal variations in HM pollution levels. Cytotoxicity was assessed in the HaCaT human keratinocyte model to assess potential relevance to human health. The pronounced exposure time- and sampling season-dependent impacts observed indicate that river water-induced toxicity is highly dynamic and robustly influenced by seasonal variations in environmental conditions. Similar to previous reports demonstrating region-specific HM accumulation patterns in aquatic ecosystems (Praveen et al., 2016; Shetaia et al., 2023), the findings of the present study suggest that seasonal fluctuations in contaminant inputs critically shape responses in biological systems.

The elevated cytotoxicity induced by autumn- and spring-collected samples is likely linked to elevations in the pollutant loads of river systems caused by surface runoff and leaching. During these

periods, fertilizers, pesticides, and industrial residues are well-recognized contributors to freshwater contamination, and their biological relevance is reflected in the substantial accumulation of multiple elements within cells detected by ICP-MS. Rapid uptake of Fe, Al, Cr, Ni, Ca, and Sr within the first 24 h suggests an early cell response to environmental exposure. In contrast, the delayed accumulation of Ti, Mn, Zn, Cu, and P at 48 h underscores the amplification in toxic effects induced by prolonged exposure.

Among the elements analyzed, Ca and Sr displayed a particularly pronounced time–season interaction. Given the central role of Ca in cell signaling, mitochondrial regulation, and membrane stability, a dysregulation in intracellular Ca accumulation may intensify cytotoxicity-associated pathways. The parallel increase in Sr, which is chemically similar to Ca, may further interfere with Ca-dependent cellular processes. These observations support the notion that Ca and Sr may function as sensitive cell-level indicators of the influence of seasonal environmental variability and pollutant pressure.

The biological relevance of HM accumulation was further substantiated by oxidative stress and genotoxicity endpoints. Significantly elevated ROS levels in most exposed cell groups indicate that oxidative stress represents a key mechanism underlying the observed cytotoxicity. Only a limited number of spring samples failed to induce a marked elevation in ROS production, consistent with their comparatively lower toxic profiles. Increased ROS generation was accompanied by an elevation in 8-OHdG levels, reflecting oxidative DNA damage and cumulative genotoxic impacts with prolonged exposure. These findings align with established evidence indicating that HMs exert genotoxicity through ROS-mediated mechanisms and the disruption of DNA repair pathways (Jadoon & Malik, 2017).

Exposure to HMs such as cadmium, lead, and arsenic results in oxidative stress, mitochondrial dysfunction, and apoptosis in human cells, including keratinocytes (Davodpour et al., 2019; Habibi et al., 2022; Li et al., 2022; Mohamed et al., 2024; Sobhanardakani, 2017, 2019).

Moreover, elevated contents of oxidative DNA damage markers, including 8-OHdG, have been detected in individuals exposed to contaminated water or HMs (Mohod & Dhote, 2013; Szymańska-Chabowska et al., 2009). The results of the present study are therefore consistent with existing toxicological evidence linking exposure to metal-contaminated environments and adverse human health outcomes.

The genotoxic potential of HMs observed in this study is further supported by similar findings made in plant and aquatic organism models, where exposure to HM-contaminated waters has been associated with chromosomal aberrations, micronuclei formation,

and DNA fragmentation (Cavusoglu et al., 2010; Chatterjee & Chatterjee, 2000; Doğan et al., 2022; Scaloni et al., 2010). Such cross-species consistency reinforces the ecological and biological relevance of the oxidative and genotoxic responses detected in HaCaT cells.

Although cadmium has been recognized as the predominant ecological threat in certain aquatic environments (Shetaia et al., 2023), the present study identified a region-specific contamination profile dominated by Fe, Al, Cr, and Ni. Such a discrepancy highlights that toxicity induced by polluted freshwater cannot be generalized across regions and underscores the necessity of site-specific assessments that consider local anthropogenic activities and environmental conditions.

Overall, the present findings demonstrate that seasonal variations in river water pollution exert significant cytotoxic and genotoxic impacts through oxidative stress-mediated mechanisms. Rather than reiterating contamination levels, these results emphasize the broader implications of sustained and seasonally-modulated pollutant exposure for human health and ecosystem integrity. Consistent with previous calls for comprehensive monitoring of metal-contaminated aquatic systems (Shetaia et al., 2023), this study underscores the importance of continuous, region-specific monitoring strategies and targeted mitigation policies addressing both agricultural and industrial sources of pollution.

Conclusion

This study comprehensively investigates the toxicity levels of river waters sampled at various locations, focusing on their impacts on human skin cells at the physiological and molecular levels. The findings offer valuable insights into the harmful effects of water pollution on human health, specifically highlighting the toxicological risks posed by HM-contaminated water. Our research demonstrates that exposure to HM-polluted river water induces significant levels of oxidative stress, DNA damage, and genotoxicity in human skin cells. Moreover, these effects varied in extent across seasons and exposure durations, underscoring the dynamic nature of water contamination and its impact on biological systems. Among the HMs analyzed, Al, Fe, and Cr were identified as key inducers of DNA damage, suggesting that these metals may serve as potential biomarkers for assessing toxicity in human skin cells. The study emphasizes the need for continuous water quality monitoring, especially in regions affected by industrial and agricultural pollutants, and advocates for further research into the mechanisms underlying HM-induced toxicity. These findings are crucial for developing effective strategies to mitigate the health risks associated with contaminated water and for advancing the protection of public health in the face of growing environmental challenges.

Table 7. Summary of t-test results applied to the ROS levels detected at 24 & 48 h of treatment vs. control. The table summarizes the results of the independent samples t-test comparing the ROS levels in HaCaT cells treated for 24 and 48 h with those of the untreated cells. The groups marked with an asterisk (*) indicate highly statistically significant differences in ROS levels, based on the threshold of $p < 0.005$. Only the E2-Spring, M1-Spring, and T3-Spring samples failed to induce ROS synthesis with statistically significant variations at this threshold.

	Levene's test for equality of variances		t-test for equal means		
	F	Sig.	t	df	Sig. (2-tailed)
E1-Autumn*	2.408	0.196	-15.724	4	0.000
E1-Winter*	2.616	0.181	15.810	4	0.000
E1-Spring*	0.304	0.610	-17.746	4	0.000
E1-Summer*	0.390	0.566	4.367	4	0.012
E2-Autumn*	1.570	0.278	20.052	4	0.000
E2-Winter*	0.683	0.455	10.046	4	0.001
E2-Spring	0.079	0.792	-0.422	4	0.695
E2-Summer*	2.441	0.193	-10.482	4	0.000
E3-Autumn*	2.176	0.214	10.177	4	0.001
E3-Winter*	1.354	0.309	3.294	4	0.030
E3-Spring*	1.409	0.301	8.280	4	0.001
E3-Summer*	0.412	0.556	-3.029	4	0.039
M1-Autumn*	1.009	0.372	16.756	4	0.000
M1-Winter*	0.324	0.600	19.103	4	0.000
M1-Spring	0.152	0.717	-1.340	4	0.251
M1-Summer*	1.371	0.307	16.610	4	0.000
M2-Autumn*	2.423	0.195	-9.515	4	0.001
M2-Winter*	0.331	0.596	18.793	4	0.000
M2-Spring*	1.411	0.301	5.458	4	0.005
M2-Summer*	0.348	0.587	-4.185	4	0.014
M3-Autumn*	3.385	0.140	-10.082	4	0.001
M3-Winter*	2.833	0.168	-13.119	4	0.000
M3-Spring*	1.111	0.351	-4.856	4	0.008
M3-Summer*	3.908	0.119	-71.920	4	0.000
T1-Autumn*	0.148	0.720	4.113	4	0.015
T1-Winter*	1.888	0.241	17.811	4	0.000
T1-Spring*	0.614	0.477	-4.061	4	0.015
T1-Summer*	1.313	0.316	3.640	4	0.022
T2-Autumn*	0.248	0.645	4.187	4	0.014
T2-Winter*	3.301	0.143	-13.406	4	0.000
T2-Spring*	0.245	0.647	5.010	4	0.007
T2-Summer*	3.800	0.123	-23.763	4	0.000
T3-Autumn*	3.312	0.143	-18.117	4	0.000
T3-Winter*	2.299	0.204	-14.474	4	0.000
T3-Spring	0.635	0.470	2.458	4	0.070
T3-Summer*	0.068	0.807	-15.962	4	0.000

HaCaT = human keratinocyte cell line; ROS = reactive oxygen species; Sig. = significance.

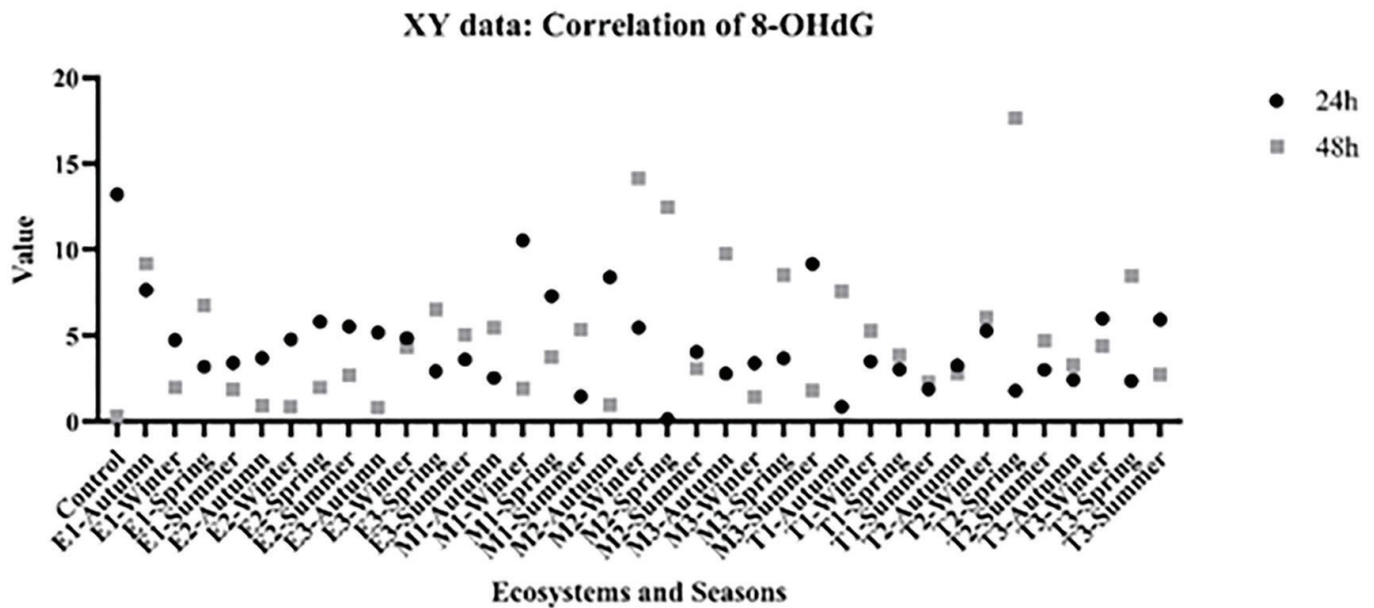


Figure 4. Oxidative DNA damage levels (8-OHdG) in HaCaT cells following river water exposure.

Levels of the oxidative DNA damage marker 8-OHdG in HaCaT cells after 24 h (black circles) and 48 h (grey squares) of exposure to river water samples categorized by ecosystem and season. The values represent arbitrary units, such as ng DNA.

8-OHdG = 8-hydroxy-2'-deoxyguanosine; HaCaT = human keratinocyte cell line.

Ethics

Ethics Committee Approval: Not required.

Data Sharing Statement: All data are available within the study.

Footnotes

Authorship Contributions:

Conceptualization: N.P.T. and P.A.M.; Design/methodology: N.P.T. and P.A.M.; Execution/investigation: N.P.T. and P.A.M.; Resources/materials: N.P.T. and P.A.M.; Data acquisition: N.P.T. and P.A.M.; Data analysis/interpretation: N.P.T. and P.A.M.; Writing – original draft: N.P.T. and P.A.M.; Writing – review & editing/critical revision: N.P.T. and P.A.M.

Conflict of Interest: The author(s) have no conflicts of interest to declare.

Funding: No external funding acquired.

Chatterjee, J., & Chatterjee, C. (2000). Phytotoxicity of cobalt, chromium and copper in cauliflower. *Environmental Pollution*, 109(1), 69–74. [https://doi.org/10.1016/s0269-7491\(99\)00238-9](https://doi.org/10.1016/s0269-7491(99)00238-9)

Chen, B., Wang, M., Duan, M., Ma, X., Hong, J., Xie, F., & Li, X. (2019). In search of key: Protecting human health and the ecosystem from water pollution in China. *Journal of Cleaner Production*, 228, 101–111. <https://doi.org/10.1016/j.jclepro.2019.04.228>

Chowdhary, P., Bharagava, R. N., Mishra, S., & Khan, N. (2019). Role of industries in water scarcity and its adverse effects on environment and human health. In *Environmental concerns and sustainable development: Volume 1: Air, water and energy resources* (pp. 235–256). Singapore: Springer Singapore. https://doi.org/10.1007/978-981-13-5889-0_12

Davodpour, R., Sobhanardakani, S., Cheraghi, M., Abdi, N., & Lorestani, B. (2019). Honeybees (*Apis mellifera* L.) as a potential bioindicator for detection of toxic and essential elements in the environment (case study: Markazi Province, Iran). *Archives of Environmental Contamination and Toxicology*, 77(3), 344–358. <https://doi.org/10.1007/s00244-019-00634-9>

Doğan, M., Çavuşoğlu, K., Yalçın, E., & Acar, A. (2022). Comprehensive toxicity screening of Pazarsuyu stream water containing heavy metals and protective role of lycopene. *Scientific Reports*, 12(1), 16615. <https://doi.org/10.1038/s41598-022-21081-y>

Fleisher, J. M., & Kay, D. (2006). Risk perception bias, self-reporting of illness, and the validity of reported results in an epidemiologic study of recreational water associated illnesses. *Marine Pollution Bulletin*, 52(3), 264–268. <https://doi.org/10.1016/j.marpolbul.2005.08.019>

Ge, J., Pitman, A. J., Guo, W., Zan, B., & Fu, C. (2020). Impact of revegetation of the Loess Plateau of China on the regional growing season water balance. *Hydrology and Earth System Sciences*, 24(2), 515–533. <https://doi.org/10.5194/hess-24-515-2020>

References

- Amaechi, M., Onuoha, D. C., & Onwuka, S. U. (2025). Analysis of seasonal variation of heavy metals concentration in selected river in Anambra State resulting from industrial effluents discharge. *Tropical Built Environment Journal*, 11(1). <https://www.tbejournal.com/index.php/tbej/article/view/163>
- Arif, A., Malik, M. F., Liaqat, S., Aslam, A., Mumtaz, K., Afzal, A., & Javed, R. (2020). Water pollution and industries. *Pure and Applied Biology (PAB)*, 9(4), 2214–2224. <https://doi.org/10.19045/bspab.2020.90237>
- Cavusoglu, K., Yapar, K., Kinalioglu, K., Turkmen, Z., Cavusoglu, K., & Yalcin, E. (2010). Protective role of Ginkgo biloba on petroleum wastewater-induced toxicity in *Vicia faba* L.(Fabaceae) root tip cells. *Journal of Environmental Biology*, 31(3), 319. <https://doi.org/10.19045/bspab.2020.90237>

- Habibi, H., Sobhanardakani, S., Cheraghi, M., Lorestani, B., & Sadr, M. K. (2022). Analysis, sources and health risk assessment of trace elements in street dust collected from the city of Hamedan, west of Iran. *Arabian Journal of Geosciences*, 15(2), 168. <https://doi.org/10.1007/s12517-022-09460-1>
- Hammoumi, D., Al-Aizari, H. S., Alaraidh, I. A., Okla, M. K., Assal, M. E., Al-Aizari, A. R., & Bejjaji, Z. (2024). Seasonal variations and assessment of surface water quality using water quality index (WQI) and principal component analysis (PCA): A case study. *Sustainability*, 16(13), 5644. <https://doi.org/10.3390/su16135644>
- Hanif, M. A., Miah, R., Islam, M. A., & Marzia, S. (2020). Impact of Kapotaksha river water pollution on human health and environment. *Progressive Agriculture*, 31(1), 1–9. <https://doi.org/10.3329/pa.v31i1.48300>
- Jadoon, S., & Malik, A. D. N. A. (2017). DNA damage by heavy metals in animals and human beings: An overview. *Biochem Pharmacol*, 6(3), 1–8. <https://doi.org/10.4172/2167-0501.1000235>
- Kazi, T. G., Arain, M. B., Baig, J. A., Jamali, M. K., Afridi, H. I., Jalbani, N., & Niaz, A. (2009). The correlation of arsenic levels in drinking water with the biological samples of skin disorders. *Science of the Total Environment*, 407(3), 1019–1026. <https://doi.org/10.1016/j.scitotenv.2008.10.013>
- Kolawole, T. A., Palacios, J., Husaini, D. C., & Nwokocha, C. R. (2025). Inflammation and oxidative stress biomarkers in heavy metal toxicity: Bridging the gap to personalized clinical interventions. *Journal of Applied Toxicology*. <https://doi.org/10.1002/jat.4874>
- Li, J. Y., Cui, D. L., Xie, Y. M., Su, J. Z., Zhang, M. Y., Niu, Y. Y., & Xiang, P. (2022). Mechanisms of Cd-induced cytotoxicity in normal human skin keratinocytes: Implication for human health. *International Journal of Molecular Sciences*, 23(19), 11767. <https://doi.org/>
- Lu, Y., Song, S., Wang, R., Liu, Z., Meng, J., Sweetman, A. J., & Wang, T. (2015). Impacts of soil and water pollution on food safety and health risks in China. *Environment International*, 77, 5–15. <https://doi.org/>
- Mohamed, A., Mahathi, P., Nair, N., & DSouza, H. (2024). The toxic effects of lead nitrate on human keratinocytes (HaCaT). *bioRxiv*, 2024-11. <https://doi.org/>
- Mohod, C. V., & Dhote, J. (2013). Review of heavy metals in drinking water and their effect on human health. *International Journal of Innovative Research in Science, Engineering and Technology*, 2(7), 2992–2996. <https://doi.org/>
- Moss, B. (2008). Water pollution by agriculture. *Philosophical Transactions of the Royal Society B: Biological Sciences*, 363(1491), 659–666. <https://doi.org/10.1098/rstb.2007.2176>
- Parris, K. (2011). Impact of agriculture on water pollution in OECD countries: Recent trends and future prospects. *Water Quality Management*, 33–52. <https://doi.org/10.1080/07900627.2010.531898>
- Payment, P., Siemiatycki, J., Richardson, L., Renaud, G., Franco, E., & Prevost, M. (1997). A prospective epidemiological study of gastrointestinal health effects due to the consumption of drinking water. *International Journal of Environmental Health Research*, 7(1), 5–31. <https://doi.org/10.1080/09603129773977>
- Praveen, P. K., Ganguly, S., Kumar, K., & Kumari, K. (2016). Water pollution and its hazardous effects to human health: A review on safety measures for adoption. *International Journal of Science, Environment and Technology*, 5(3), 1559–1563. https://www.researchgate.net/publication/303698187_water_pollution_and_its_hazardous_effects_to_human_health_a_review_on_safety_measures_for_adoption
- Scalon, M. C. S., Rechenmacher, C., Siebel, A. M., Kayser, M. L., Rodrigues, M. T., Maluf, S. W., & Silva, L. B. D. (2010). Evaluation of Sinos River water genotoxicity using the comet assay in fish. *Brazilian Journal of Biology*, 70, 1217–1222. <https://doi.org/10.1590/s1519-69842010000600011>
- Shetaia, S. A., Nasr, R. A., El Saeed, R. L., Dar, M. A., Al-Mur, B. A., & Zakaly, H. M. (2023). Assessment of heavy metals contamination of sediments and surface waters of Bitter lake, Suez Canal, Egypt: Ecological risks and human health. *Marine Pollution Bulletin*, 192, 115096. <https://doi.org/10.1016/j.marpolbul.2023.115096>
- Sobhanardakani, S. (2017). Potential health risk assessment of heavy metals via consumption of caviar of Persian sturgeon. *Marine Pollution Bulletin*, 123(1-2), 34–38. <https://doi.org/10.1016/j.marpolbul.2017.09.033>
- Sobhanardakani, S. (2019). Ecological and human health risk assessment of heavy metal content of atmospheric dry deposition, a case study: Kermanshah, Iran. *Biological Trace Element Research*, 187(2), 602–610. <https://doi.org/10.1007/s12011-018-1383-1>
- Szymańska-Chabowska, A., Beck, A., Poręba, R., Andrzejak, R., & Antonowicz-Juchniewicz, J. (2009). Evaluation of DNA damage in people occupationally exposed to arsenic and some heavy metals. *Polish Journal of Environmental Studies*, 18(6). <https://www.pjoes.com/pdf-88337-22195?filename=Evaluation%20of%20DNA%20Damage.pdf>
- Wu, C., Maurer, C., Wang, Y., Xue, S., & Davis, D. L. (1999). Water pollution and human health in China. *Environmental Health Perspectives*, 107(4), 251–256. <https://doi.org/10.1289/ehp.99107251>
- Wu, H., Gai, Z., Guo, Y., Li, Y., Hao, Y., & Lu, Z. N. (2020). Does environmental pollution inhibit urbanization in China? A new perspective through residents' medical and health costs. *Environmental Research*, 182, 109128. <https://doi.org/10.1016/j.envres.2020.109128>
- Xiao, J., Wang, L., Deng, L., & Jin, Z. (2019). Characteristics, sources, water quality and health risk assessment of trace elements in river water and well water in the Chinese Loess Plateau. *Science of the Total Environment*, 650, 2004–2012. <https://doi.org/10.1016/j.scitotenv.2018.09.322>
- Yassin, M. M., Amr, S. S. A., & Al-Najar, H. M. (2006). Assessment of microbiological water quality and its relation to human health in Gaza Governorate, Gaza Strip. *Public Health*, 120(12), 1177–1187. <https://doi.org/10.1016/j.puhe.2006.07.026>
- Yau, V., Wade, T. J., de Wilde, C. K., & Colford Jr, J. M. (2009). Skin-related symptoms following exposure to recreational water: A systematic review and meta-analysis. *Water Quality, Exposure and Health*, 1(2), 79–103. <https://link.springer.com/article/10.1007/s12403-009-0012-9>